Frontiers in Engineering and Informatics
ISSN: 3049-3412 (Online)
Volume No: 01 – Issue No: 02 – June 2025

A Dual Attention Holographic Convolutional Neural Network with Perfumer Optimization Algorithm for Accurate Brain Tumor Detection Using MRI Images

N Saravanan[1]*, Harsha Singh[2]

[1]*Department of Biotechnology, Muthayammal Engineering College (Autonomous), Rasipuram – 637108, Namakkal, Tamil Nadu, India.

[2]Department of Computer Science and Engineering, RK College of Engineering (Autonomous), GURUKUL SCHOOL ROAD, Zami Machavaram, Andhra Pradesh 521456, India.

[1*]coe@mec.edu.in,[2]harshasinghrkce@gmail.com

Corresponding author E-mail ID: coe@mec.edu.in

Abstract :

The classification of Brain Tumor (BT) based on MRI images is one of the most crucial tasks in medical imaging because proper diagnosis directly influences the early treatment planning and patient survival. Although deep learning has made progress, it still experiences difficulties with accurate tumor segmentation, boundary preservation, and accurate differentiation of features across different tumor grades. In order to overcome these shortcomings, the proposed Dual Attention Holographic Convolutional Neural Network with Perfumer Optimization Algorithm (DAHCNNet-POA) offers a strong baseline of automated BT classification. The MRI images are first acquired on the BraTS 2018 dataset. Shape-Aware Mesh Normal Filtering (S-AMNF) is applied to perform preprocessing that removes noise without losing the structural and boundary integrity. A Visual Geometry Grounded Transformer (VGGT) is used to segment tumor regions accurately and capture both spatial and geometric relationships. After that, the discriminative features are obtained and classified in the DAHCNNet, which incorporates both spatial and channel attention to improve the learning of the representation. The network weights are optimized through POA, which enhances convergence and performance. The model got 99.12% accuracy of HGG, 99.18% accuracy of LGG, and Dice scores greater than 99, which proved its high reliability and effectiveness.

Keywords: *Brain tumor classification, Dual Attention Holographic Convolutional Neural Network, Perfumer Optimization Algorithm, Visual Geometry Grounded Transformer, Tumor segmentation.*

1. INTRODUCTION

A brain tumor (BT) is a pathological proliferation of brain cells, which may be either benign or malignant. They can grow in the brain (primary), or they can be transferred to the brain through other

DoI: https://doi.org/10.63949/crinfo.v1i2.002

body parts (metastatic) Rahman, T et al, (2023). Meningioma, Glioma, and Pituitary tumors are the common types of tumors with their own symptoms that include headaches, vomiting, and neurological disorders Aggarwal, M et al, (2023). Proper diagnosis and categorization of BTs are necessary in order to plan treatment. Noninvasive visualization of abnormalities of the brain is commonly done by use of Magnetic Resonance Imaging (MRI). T1, T2, T1-contrast, and FLAIR modalities of MRI can give detailed pathological and structural data Rasheed, Z et al, (2023). The recent breakthrough in deep learning, especially convolutional neural networks (CNNs) and transfer learning, has demonstrated considerable enhancement of the accuracy of automated tumor detection, as well as classification Alshuhail, A et al, (2024).

Detection and classification of brain tumors in MRI scans is tedious and time-consuming to do manually, and prone to error, particularly with large datasets. Tumors are diverse in terms of size, shape, localization, and intensity, and it is difficult to diagnose them in a consistent manner Preetha, R. et al, (2024). Conventional procedures are usually unable to deal with complicated tumor features and variations under varying imaging conditions, resulting in inconsistent findings. Even though deep learning methods have reached a high level of accuracy, multi-class problems, efficient feature extraction, and transfer to new data continue to be challenges Abdusalomov, A.B. et al, (2023). Slowness or errors in the detection of the tumor may have a direct effect on the treatment results and survival of the patient. Hence, there is a great demand for reliable and automated systems that can analyze MRI scans effectively, segregate tumors, and offer effective classification Asiri, A.A. et al, (2024).

The timely and accurate diagnosis of brain tumors can lead to a much better patient outcome and be helpful in making treatment choices. The MRI diagnostic systems developed through automation avoid the need to use manual interpretation systems, hence avoiding errors and also improving clinical procedures. The deep learning models and transfer learning are also highly successful in the extraction of meaningful features and the high-accuracy classification of tumors. These systems are capable of dealing with large datasets, ensuring consistency among various imaging conditions, and assisting clinicians with decision-making. Thus, the proposed research aims to create a deep learning-based model that can be used to classify brain tumors and enhance the quality of diagnostics and efficiency.

Novelty and Contributions

- This paper presents a new Dual Attention Holographic Convolutional Neural Network with Perfumer Optimization Algorithm (DAHCNNet-POA) to directly classify brain tumors by combining the three representations of spatial, channel, and holographic features.
- A preprocessing strategy is based on an S-AMNF that is capable of eliminating noise effectively, maintaining fine tumor boundaries, and structural features of MRI images.
- A VGGT-based segmentation framework is adopted to localize tumor areas accurately by training long-range spatial and geometric correlation.

DoI: https://doi.org/10.63949/crinfo.v1i2.002

- The proposed DAHCNNet combines holographic convolution and a dual-attention mechanism to obtain highly discriminative and rotation-resistant tumor features to enable reliable classification.
- An algorithm called Perfumer Optimization Algorithm (POA) is added as an adaptive weight optimization method, and it allows balanced exploration and exploitation, more rapid convergence, and better classification accuracy.

The relevant literature is carefully assessed in Section 2. Section 3 provides a detailed explanation of the techniques used in this study. Section 4 discusses the outcome and its implications. Personal reflections and recommendations for additional research are included in Section 5.

2. Literature Survey

Sharif et al. proposed the optimized deep learning-based classification of BT in 2024. Contrast enhancement was performed using Hybrid Division Histogram Equalization (HDHE) with the Ant Colony Optimization (ACO) technique and a nine-layer CNN. The Differential Evolution (DE) and Moth Flame Optimization (MFO) were used to optimize features of the Fully Connected (FC) layer, and the Multi-Class Support Vector Machine (MC-SVM) was used to classify features. It was more accurate, but not as easy, as computational complexity was also a factor.

In 2024, Sachdeva et al. then presented a multiscale Efficient-Residual Network on BT classification based on MRI. The algorithm was a combination of the deep features of the ResNet50 and EfficientNetB0 models, where skip connections and compound scaling were used to improve the learning of representations. The procedure enhanced the separation of tumors of complicated structure. Better robustness and generalization in various imaging conditions were the primary benefits. One of the weaknesses was the greater complexity of models and the augmented computational needs to deploy.

In 2023, Haqu et al. implemented fast approaches to BT detection using MRI, which are based on fast deep learning. Two CNN-based architectures were created to classify the type of tumor and discriminate the grade of Glioma. Segmentation outputs were optimized with intensity normalization, data augmentation, and Conditional Random Fields (CRF). The solution saved manual labor and enhanced efficiency in diagnostics. One of the main benefits was proper automated classification, but sensitivity to image quality was a weakness.

In 2023, Cao et al. introduced a three-dimensional Multi-Branch Attention Network (3D MBANet) that would segment brain tumors using MRI. The technique combined the optimized Shuffle Units and multi-branch 3D Shuffle Attention, as incorporated in the encoder and skip connections to learn the spatial and channel context. The procedure improved multimodal features representations and segmentation accuracy. The significant benefit was the better boundary delineation, whereas high memory consumption and computation were significant drawbacks.

DoI: https://doi.org/10.63949/crinfo.v1i2.002

2.1 Problem Statement

The classification of brain tumors based on MRI images is a difficult undertaking because of the heterogeneous nature of the tumors, variations in size, shape, and location, low contrast, and noise in the MRI images. Conventional techniques tend to be ineffective in segmenting the tumor edges and finding those characteristics that are discriminative, thus leading to poor classification results. Besides, the current deep learning models can also be associated with overfitting and sluggish convergence with complex multimodal MRI data. The challenges encourage the creation of a strong and optimized scheme of accurate and dependable automated BT classification.

3. Proposed Methodology

This part outlines the proposed Dual Attention Holographic Convolutional Neural Network with Perfumer Optimization Algorithm (DAHCNNet-POA) to classify brain tumors. Initially, the brain MRI images are taken using the BraTS 2018 data series, which entails multimodal and annotated tumor images. The obtained images are further preprocessed through Shape-Aware Mesh Normal Filtering (S-AMNF), which minimizes noise without affecting the structural and boundary information. Subsequent to preprocessing, precise tumor regions are identified using a Visual Geometry Grounded Transformer (VGGT) based segmentation by training on spatial relationships and geometric relationships. The discriminative features are then identified and categorized with the help of the Dual Attention Holographic Convolutional Neural Network (DAHCNNet) that incorporates both spatial and channel attention to learn better representations. Lastly, the Perfumer Optimization Algorithm (POA) is used to optimally tune the network weights in order to enhance convergence and classification. The proposed DAHCNNet-POA architecture is described in Figure 1.

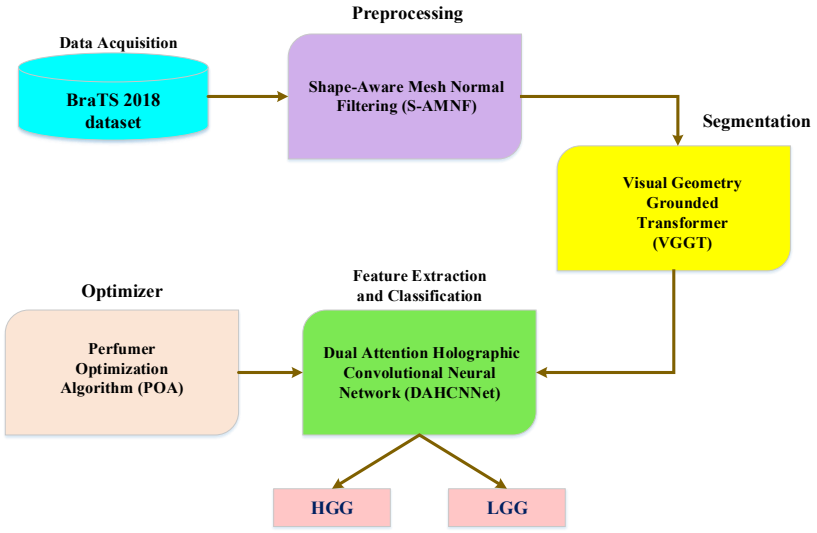

Figure 1. Proposed Architecture

DoI: https://doi.org/10.63949/crinfo.v1i2.002

3.1 Data Acquisition

The BraTS 2018 dataset is used for data acquisition, which involves acquiring multimodal brain Magnetic Resonance Imaging (MRI) scans with varied tumor characteristics. Through data acquisition, images are obtained, and also include clinical annotations of the tumor region for analysis. The dataset follows standardized image acquisition procedures, ensuring the images are from similar conditions. The obtained brain Magnetic Resonance Imaging images undergo preprocessing, including eliminating noise, normalizing intensities, resizing, and image enhancement.

3.2 Preprocessing using Shape-Aware Mesh Normal Filtering (S-AMNF)

S-AMNF Zhong, S et al, (2021) applies as image preprocessing for the purpose of enhancing structural consistency with reduced noise. For every local region, guidance normal H_j is computed using shape-aware patches to keep the significant geometric details, which is expressed as equation (1).

$$H_j = \Gamma\left(\sum_{k \in Q_j} b_k M_k\right) \tag{1}$$

where, Q_j denotes the local patch, M_k represents the normal of neighboring region k, b_k is the corresponding area weight, and Γ indicates normalization. Given by Equation (2), a patch consistency measure is defined in order to select reliable patches.

$$S(Q_j) = G(Q_j) \bullet T(Q_j) \tag{2}$$

where, $S(Q_j)$ is the total consistency score of patch Q_j. $G(Q_j)$ measures the flatness of the patch by computing both the local and global variations within the considered region, while $T(Q_j)$ quantifies the orientation similarity between the central region and its neighboring regions. A lesser value of $S(Q_j)$ means that the patch will be smoother and more consistent after preprocessing. The enhanced images after S-AMNF preprocessing undergo segmentation with accuracy in tumor region delineation.

3.3 Segmentation using Visual Geometry Grounded Transformer (VGGT)

Segmentation is done via the VGGT Wang, J. et al, (2025), which processes the sequence of input images and jointly learns the geometric and spatial representations. Given a set of N input images, VGGT maps each image to corresponding geometric outputs, as given in Equation (3):

DoI: https://doi.org/10.63949/crinfo.v1i2.002

Frontiers in Engineering and Informatics
ISSN: 3049-3412 (Online)
Volume No: 01 – Issue No: 02 – June 2025

$$g\left(\left(J_j\right)_{j=1}^{M}\right)=\left(h_j,E_j,Q_j,U_j\right)_{j=1}^{M} \quad (3).$$

where, g is the VGGT transformer that maps each input image, J_j is the input image, h_j denotes the estimated camera parameters including rotation, translation, and field of view, E_j is the depth map providing pixel-wise spatial information, Q_j is the 3D point map aligned in a common reference frame, and U_j represents dense feature maps preserving spatial correspondences. M stands for the total number of input images within one sequence. By incorporating an alternating frame-wise and global self-attention mechanism, VGGT captures not only local tumor boundary information but also global structural context of critical value for accurate segmenting of tumor regions. Features are extracted after segmentation from those segmented regions and used directly to classify the tumor type.

3.4 Feature Extraction and Classification using Dual Attention Holographic Convolutional Neural Network (DAHCNNet)

The Dual Attention Holographic Convolutional Neural Network (DAHCNNet) Wu, K. et al, (2023), Pun, M.N. et al, (2024) is employed for feature extraction and classification of brain tumors after the segmentation of MRI images. The DAHCNNet is a blend of a Dual Attention Transformer Network (DATN) and a Holographic Convolutional Neural Network (H-CNN) and is capable of extracting hierarchical spatial features and structure information of the BT structure. $J_t \in \Re^{h\times w\times c}$ is the tumor region of the MRI image. The segmented map of the image is first converted to the feature domain by using a convolution layer with LeakyReLU activation, and this is expressed by equation (4).

$$J_0 = g_{in}\left(J_t\right) \quad (4).$$

where J_0 is the feature map obtained, g_{in} is a 3×3 convolution layer with LeakyReLU activation, and J_t is the segmented tumor image with a height of h, a width of w, and c channels. The feature map is then passed to the encoder DAT modules, which is shown in Equation (5).

$$J_j = E_j\left(DAT_j\left(J_{j-1}\right)\right), \quad j=1-3 \quad (5).$$

where DAT_j represents the j^{th} module in the Dual-Attention Transformer that focuses on both the spatial and the channel aspects, E_j represents the downsampling block that uses 4×4 convolutional

DoI: https://doi.org/10.63949/crinfo.v1i2.002

layers with stride 2, and the output of this module results in J_j, the feature map from the encoder. The RestBottleneck modules enhance the abstract representation generated from the features described by equation (6).

$$J_j = DAT_j\left(J_{j-1}\right), \qquad j = 4,5 \tag{6}.$$

Where, $j = 4,5$ represent the two DAT modules in the bottleneck enhancing contextual tumor features. In the decoder, feature maps are upsampled and merged with skip connections from the encoder, as expressed in Equation (7).

$$J_j = DAT_j\left(V_j\left(J_{j-1}\right), J_{9-j}\right), \qquad J = 6-8 \tag{7}.$$

Where, V_j is the upsampling sub-graph using transposed convolutions at 2×2 sizes with stride 2, while J_{9-j} is the encoder feature map via skip connections. Finally, the tissue feature map in Equation (8) is calculated.

$$G_{tumor} = g_{out}\left(J_8\right) + L_{\uparrow} \tag{8}.$$

where g_{out} is a 3×3 convolutional layer $L_{\uparrow}$ to produce the high-resolution feature map used in classification G_{tumor}. For tumor classification tasks, the H-CNN model encodes 3D structure properties in the segmented region of interest as characterized in Equation (9).

$$A = H - CNN(y) \tag{9}.$$

Where, y is the volume of the divided tumor, and A is the weight feature vector that captures the intensity and structural characteristics of the tumor. The classification is done using Equation (10).

$$\Delta \log Q = \log \frac{Q_{class}}{Q_{others}} \tag{10}.$$

where, Q_{class} is the probability of the true tumor class, Q_{others} are the probabilities of other tumor classes, and $\Delta \log Q$ is the log-ratio employed for robust classification. The proposed DAHCNNet approach leverages the hierarchical feature extraction technique of the DATN algorithm and the tumor

DoI: https://doi.org/10.63949/crinfo.v1i2.002

representation of the H-CNN architecture to efficiently extract identifiable features and classify brain tumors while preserving fine details.

3.5 DAHCNNet optimizer using Perfumer Optimization Algorithm (POA)

DAHCNNet utilizes the POA Hamadneh, T. et al, (2025) to optimize network weights for better feature extraction and classification. POA takes inspiration from the methodology of a perfumer during the creation of a fragrance, which requires exhaustive exploration to scan the weight space broadly or effectively narrow down to fine-tune promising solutions. Each candidate solution represents one set of DAHCNNet weights, to be iteratively updated with the aim of improving performance. Such a two-phase optimization ensures robust convergence, avoids local minima, and thereby enhances the classification accuracy that makes DAHCNNet effective for BT detection. The POA is described in Algorithm 1.

Algorithm 1: DAHCNNet weight optimization using POA

Initialize population Y with M candidate weight solutions.
Evaluate fitness function $f(Y)$ for all candidates.
Identify Y_{best} with minimum $f(Y)$
for $t = 1$ to MaxIterations do
  for $j = 1$ to M do
    $s = random(0,1)$
    $J = random_{choice}(\{1,2\})$
    // Phase 1: Exploration (broad search)
    $RF_j = Y_j + s * (Y_{best} - J * Y_{worst})$
    $Y_{new}^j = Y_j + J * s * (RF_J - J * Y_j)$
    if $f(Y_{new}^j) < f(Y_j)$
      $Y_j = Y_{new}^j$
    // Phase 2: Exploitation (fine-tuning)
    $Y_{new}^j = Y_j + (1 - 2 * J * s) * (upb - lob)/t$
    if $f(Y_{new}^j) > f(Y_j)$
      $Y_j = Y_{new}^j$
  Update Y_{best} based on the updated $f(Y)$
end for
Return Y_{best} as optimized DAHCNNet weights.

DoI: https://doi.org/10.63949/crinfo.v1i2.002

4. Results

This section discusses the experimental results of the proposed DAHCNNet-POA model to assess its effectiveness in the classification of brain tumours through MRI images. The entire architecture is executed in Python 3.9 through the use of the TensorFlow and Keras deep learning packages, supported by NumPy, Pandas, and Scikit-learn to handle, preprocess, and assess the performance. All experiments are run on a platform with an Intel Core i7 processor (2.8 GHz), 16 GB RAM, a 4 GB graphics card, and a Windows 64-bit operating system. Experimentation is performed with the BraTS 2018 dataset, in which S-AMNF, VGGT, and DAHCNNet-POA are applied in order. Table 1 summarizes the most important parameters of the simulation in the experiments.

Table 1. Simulation Parameters

Parameters	Description
Operating System	Windows 64-bit
Dataset	BraTS 2018
Data Type	MRI
Proposed Model	DAHCNNet
Optimizer	POA
Number of Epochs	100

4.1 Dataset Description

BRATS2018 https://www.kaggle.com/datasets/sanglequang/brats2018 is a benchmark dataset that includes multimodal MRI scans of brain tumors: High-grade Glioma (HGG) and Low-grade Glioma (LGG). It has a total number of 39,835 images, where 27,035 images are included in the training, and 12,800 are included in the testing. The data is formed by 29,605 HGG images (19,805 training images and 9,800 test images) and 10,230 LGG images (7,230 training images and 3,000 test images). It has been extensively applied in the analysis of tumor segmentation and classification models.

4.2 Performance Analysis

To test the effectiveness of the proposed DAHCNNet-POA model to classify brain tumors, it is applied to the BraTS 2018 dataset and compared with the existing models, such as MC-SVM Sharif, M.I et al, (2024), ResNet50 Sachdeva, J. et al, (2024), CNN, and 3D MBANet Haq, E.U. et al, (2023). The accuracy, precision, and recall, as well as the F1-score, Dice score, and Jaccard index, are used to assess the performance of HGG and LGG classes.

DoI: https://doi.org/10.63949/crinfo.v1i2.002

Frontiers in Engineering and Informatics
ISSN: 3049-3412 (Online)
Volume No: 01 – Issue No: 02 – June 2025

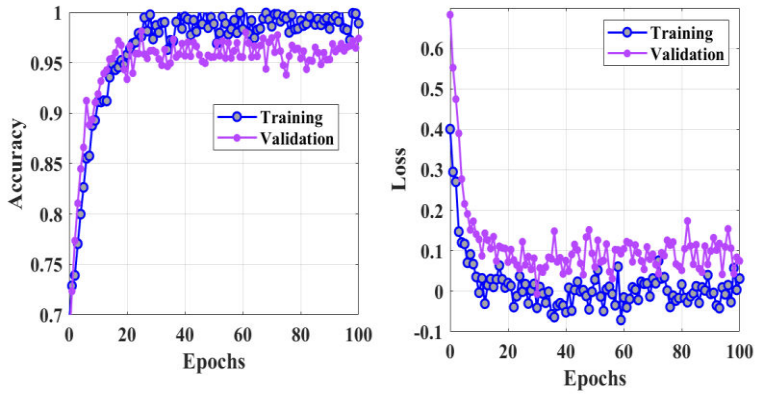

(a) **(b)**

Figure 2. (a) Accuracy (b) Loss for Proposed DAHCNNet-POA

The proposed model of training and validation accuracy curves of the proposed model, which is the DAHCNNet-POA, is plotted in Figure 2(a) with 100 epochs. The training accuracy gradually grows and reaches a constant value around 0.98, and the validation accuracy takes second place, which shows that there is a small amount of overfitting and a good generalization effect is achieved. The training and validation loss in terms of epochs is plotted in Figure 2(b) below. The training loss reaches a minimum at the early epochs, and then, it levels off to a small number, whereas the validation loss exhibits the same kind of behavior, which proves that the model has converged and is learning consistently in the case of BT classification.

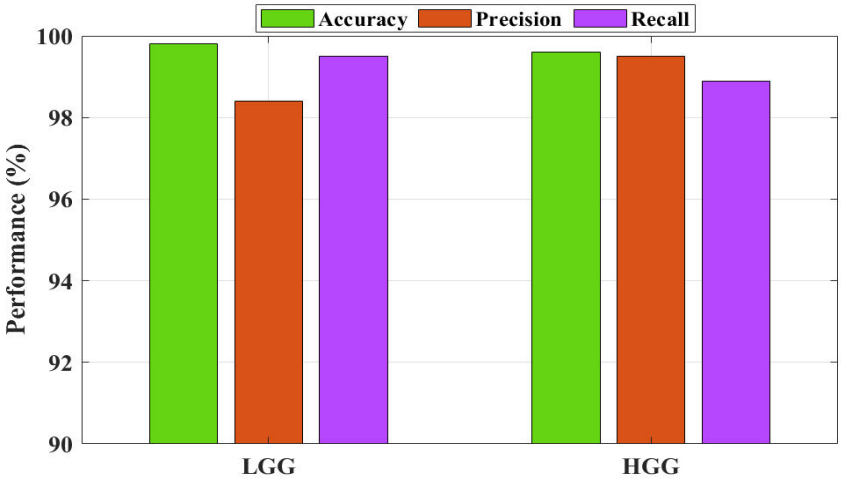

Figure 3. LGG and HGG Performance of DAHCNNet-POA

DoI: https://doi.org/10.63949/crinfo.v1i2.002

Frontiers in Engineering and Informatics
ISSN: 3049-3412 (Online)
Volume No: 01 – Issue No: 02 – June 2025

Figure 3 shows the results of the comparison of performances between LGG and HGG classes. Both tumor types have high results in terms of accuracy of above 99%, a precision of above 99% and a recall of above 99%, which indicates that the model has a good feature extractor, classification ability, and good reliability in differentiating between tumor types.

Table 2. Performance Comparison

Method	Class	Accuracy (%)	Precision (%)	Recall (%)	F1-Score (%)	Dice Score (%)	Jaccard Index (%)
MC-SVM Sharif, M.I et al, (2024)	HGG	86.12	84.35	83.78	84.06	82.91	70.89
	LGG	84.27	82.96	81.54	82.24	81.08	68.29
ResNet50 Sachdeva, J. et al, (2024)	HGG	89.45	88.12	87.36	87.74	86.95	76.92
	LGG	87.93	86.54	85.91	86.22	85.37	74.19
CNN Haq, E.U. et al, (2023)	HGG	90.31	89.06	88.74	88.90	87.82	78.22
	LGG	88.76	87.35	86.82	87.08	86.41	75.81
3D MBANet Cao, Y et al, (2023)	HGG	92.84	91.92	91.36	91.64	90.88	82.03
	LGG	91.26	90.18	89.77	89.97	89.14	80.44
Proposed DAHCNNet-POA	HGG	99.12	99.08	99.03	99.05	99.01	98.12
	LGG	99.18	99.11	99.06	99.08	99.04	98.21

Table 2 provides a performance evaluation of current and suggested HGG and LGG classification methods. MC-SVM resulted in 86.12% and 84.27% accuracies on HGG and LGG, respectively, whereas ResNet50 and CNN had moderate improvements with accuracies under 91% respectively. The 3D MBANet performance was even higher at 92.84% with HGG and 91.26% with LGG. Conversely, the proposed DAHCNNet-POA was much better at all approaches as it reached 99.12% accuracy on HGG and 99.18% on LGG, and the precision, recall, F1-score, Dice score, and Jaccard index were all above 98%.

5. Conclusion

The developed DAHCNNet-POA model showed high-quality classification of brain tumors on the BraTS 2018 dataset. The model had an accuracy of 99.12% and 99.18% for HGG and LGG, respectively, and a precision of 99.08% and 99.11% respectively. Recall (99.03% with HGG and 99.06% with LGG) and F1-scores (99.05% and 99.08%) are high, which points to the reliable tumor discrimination. Furthermore, high Dice scores (99.01% in the case of HGG and 99.04% in the case of LGG) and Jaccard indices (98.12% and 98.21%, respectively) indicate correct tumor area coverage and the distinctions in classes. The key strengths of the proposed model are effective learning of features with dual attention, global representation with holographic convolution, and weight optimization with POA, to achieve stable convergence and high accuracy. Nevertheless, the framework is more computationally expensive because of attention and transformer dimensions, and is trained on one dataset. Further development will involve

DoI: https://doi.org/10.63949/crinfo.v1i2.002

computational optimization, cross-dataset validation, and extension to multi-grade tumor analysis and clinical decision support.

REFERENCES

[1] Rahman, T., & Islam, M. S. (2023). MRI brain tumor detection and classification using parallel deep convolutional neural networks. *Measurement: Sensors*, 26, 100694.

[2] Aggarwal, M., Tiwari, A. K., Sarathi, M. P., & Bijalwan, A. (2023). Early detection and segmentation of brain tumors using deep neural networks. *BMC Medical Informatics and Decision Making*, 23(1), 78.

[3] Rasheed, Z., Ma, Y. K., Ullah, I., Ghadi, Y. Y., Khan, M. Z., Khan, M. A., Abdusalomov, A., Alqahtani, F., & Shehata, A. M. (2023). Brain tumor classification from MRI using image enhancement and convolutional neural network techniques. *Brain Sciences*, 13(9), 1320.

[4] Alshuhail, A., Thakur, A., Chandramma, R., Mahesh, T. R., Almusharraf, A., Vinoth Kumar, V., & Khan, S. B. (2024). Refining neural network algorithms for accurate brain tumor classification in MRI imagery. *BMC Medical Imaging*, 24(1), 118.

[5] Preetha, R., Priyadarsini, M. J. P., & Nisha, J. S. (2024). Automated brain tumor detection from magnetic resonance images using fine-tuned EfficientNet-B4 convolutional neural networks. *IEEE Access*.

[6] Abdusalomov, A. B., Mukhiddinov, M., & Whangbo, T. K. (2023). Brain tumor detection based on deep learning approaches and magnetic resonance imaging. *Cancers*, 15(16), 4172.

[7] Asiri, A. A., Soomro, T. A., Shah, A. A., Pogrebna, G., Irfan, M., & Alqahtani, S. (2024). Optimized brain tumor detection: A dual-module approach for MRI image enhancement and tumor classification. *IEEE Access*, 12, 42868–42887.

[8] Sharif, M. I., Li, J. P., Khan, M. A., Kadry, S., & Tariq, U. (2024). M3BTCNet: Multi-model brain tumor classification using metaheuristic deep neural network feature optimization. *Neural Computing and Applications*, 36(1), 95–110.

[9] Sachdeva, J., Sharma, D., Ahuja, C. K., & Singh, A. (2024). Efficient-Residual Net: A hybrid neural network for automated brain tumor detection. *International Journal of Imaging Systems and Technology*, 34(5), e23170.

[10] Haq, E. U., Jianjun, H., Li, K., Haq, H. U., & Zhang, T. (2023). An MRI-based deep learning approach for efficient classification of brain tumors. *Journal of Ambient Intelligence and Humanized Computing*, 14(6), 6697–6718.

[11] Cao, Y., Zhou, W., Zang, M., An, D., Feng, Y., & Yu, B. (2023). MBANet: A 3D convolutional neural network with multi-branch attention for brain tumor segmentation from MRI images. *Biomedical Signal Processing and Control*, 80, 104296.

[12] Zhong, S., Song, Z., Liu, Z., Xie, Z., Chen, J., Liu, L., & Chen, R. (2021). Shape-aware mesh normal filtering. *Computer-Aided Design*, 140, 103088.

[13] Wang, J., Chen, M., Karaev, N., Vedaldi, A., Rupprecht, C., & Novotny, D. (2025). VGGT: Visual geometry grounded transformer. In *Proceedings of the IEEE/CVF Conference on Computer Vision and Pattern Recognition (CVPR)* (pp. 5294–5306).

[14] Wu, K., Yang, X., Nie, Z., Li, H., & Jeon, G. (2023). A dual-attention transformer network for pansharpening. *IEEE Sensors Journal*, 24(5), 5500–5511.

DoI: https://doi.org/10.63949/crinfo.v1i2.002

[15] Pun, M. N., Ivanov, A., Bellamy, Q., Montague, Z., LaMont, C., Bradley, P., Otwinowski, J., & Nourmohammad, A. (2024). Learning the shape of protein microenvironments with a holographic convolutional neural network. *Proceedings of the National Academy of Sciences*, 121(6), e2300838121.

[16] Hamadneh, T., Batiha, B., Gharib, G. M., Montazeri, Z., Dehghani, M., Aribowo, W., Zalzala, A. M., Jawad, R. K., Ahmed, M. A., Ibraheem, I. K., & Eguchi, K. (2025). Perfumer optimization algorithm: A novel human-inspired metaheuristic for solving optimization tasks. *International Journal of Intelligent Engineering and Systems*, 18(4), 633–643.

[17] https://www.kaggle.com/datasets/sanglequang/brats2018

DoI: https://doi.org/10.63949/crinfo.v1i2.002